The NH_3 Mass Accommodation Coefficient for Uptake onto Sulfuric Acid Solutions

D. Hanson* and E. Kosciuch

Atmospheric Chemistry Division, National Center for Atmospheric Research, Boulder, CO 80307-3000

Received: July 9, 2002; In Final Form: October 31, 2002

The uptake of NH_3 onto particles with diameters of ∼100 nm composed of sulfuric acid and water was studied in a laminar flow reactor. The gas-phase loss of NH_3 was monitored with a chemical ionization mass spectrometer. Temperature ranged from 287 to 296.5 K. The mass accommodation coefficient, α, was found to be close to unity for NH_3 uptake onto the surface of 15−65 wt % H_2SO_4 solutions. The finding that α does not depend on composition over this range of acid content is at odds with recently published work on the same subject where the measured NH_3 mass accommodation coefficient was observed to decrease from unity on 70 wt % H_2SO_4 to 0.3(±0.05) on 20 wt % H_2SO_4. Possible reasons for this discrepancy and consequent implications for results from that experimental technique will be discussed. A value of unity for α indicates that the neutralization of sulfuric acid particles by atmospheric ammonia will be efficient.

Introduction

Ammonia plays an important role in the formation and growth of atmospheric particles. For example, recent measurements of particle nucleation[1] and $NH_3-H_2SO_4$ clusters[2] have demonstrated the important role that NH_3 vapor can have in the formation of new particles.[3,4] Also, the uptake of ammonia by sulfuric acid and nitric acid particles leads to their neutralization and stabilization; uptake of ambient ammonia onto particles is commonly inferred from observations of neutralized particles in the atmosphere.[5,6]

The mass accommodation coefficient of NH_3 describes the efficiency of uptake of ammonia onto water and sulfuric acid solutions. This process is a classic topic in the study of atmospheric heterogeneous chemistry and it has been the subject of laboratory studies over the course of ∼40 years.[7−13] Results from these experiments yield values of the mass accommodation coefficient for NH_3 that range from ∼0.1 up to unity.

We have recently performed experiments on the uptake of NH_3 onto dilute sulfuric acid solutions by observing the gas-phase loss of NH_3 in the presence of ∼100 nm diameter droplets. Gas-phase NH_3 was detected with a chemical ionization mass spectrometer (CIMS) and particle size distributions were monitored with a differential mobility analyzer. Sulfuric acid content ranged from 15−65 wt % and temperature was 287−296.5 K.

Experiment

The uptake of gas-phase NH_3 onto sulfuric acid particles was studied in a vertically aligned laminar flow reactor (i.d. of 5.17 cm and length of 120 cm) operated at atmospheric pressure (∼610 Torr). A schematic drawing of the apparatus is shown in Figure 1. The experimental procedure is much the same as described by Lovejoy and Hanson[14] and Mozurkewich et al.[15] in experiments on the reaction of N_2O_5 with sulfuric acid particles. Chemical ionization mass spectrometry was used to detect gas-phase NH_3 and a differential mobility analyzer and condensation nucleus counters were used to obtain the aerosol size distribution and number density.

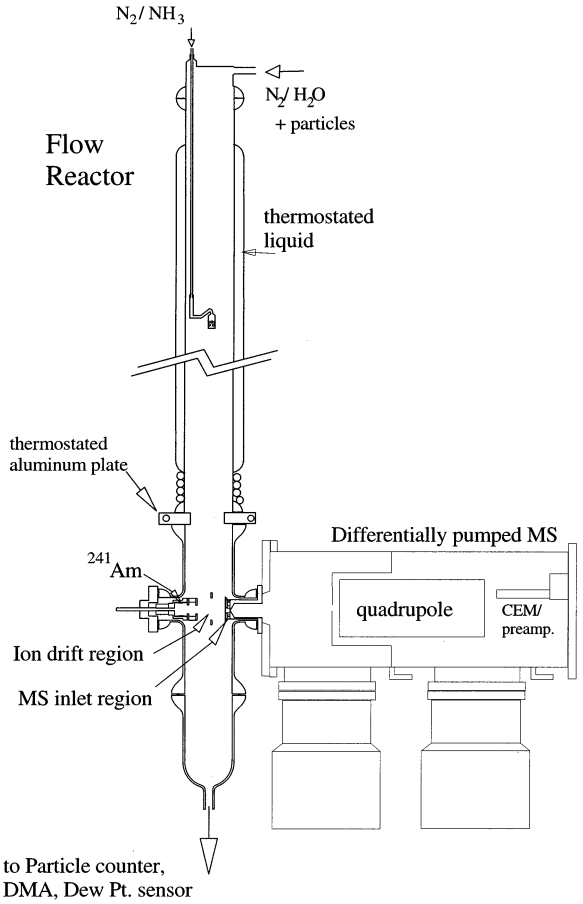

Figure 1. Schematic drawing of the vertical flow reactor, injector, and NH_3 detector. The direction of the flow is in the direction of the acceleration due to gravity.

Reactant NH_3 was introduced through a moveable injector and particles were introduced with the main flow. The NH_3 inlet at the end of the injector consisted of a 0.7 cm Teflon plug that had 8 holes (∼1 mm diameter) in its perimeter through which the N_2/NH_3 gas entered the flow reactor. A jacket for circulating cooling fluid (water, $T = 287-296$ K) surrounded all but ∼10

* Corresponding author.

10.1021/jp021570j CCC: $25.00
Published on Web 03/05/2003

cm of the reactor near its ends. The end at the exit was wrapped with flexible tubing containing the cooling fluid. A 1.2 cm thick aluminum plate with a ~4 cm i.d. hole in it was placed between the flow reactor and the detector flange. This plate was temperature regulated by circulating coolant through two 1/4-in. i.d. holes along its length. Experiments performed below room temperature without thermoregulation of this plate were affected by gas that had warmed on contact with it. The plate served to provide thermoregulation of the gas in the flow reactor all the way to its end. The gas exiting the flow reactor through the aluminum plate traveled a distance of about 10 cm to the ionization region of the detector.

Total flow rate of N_2 (taken from the gas over liquid nitrogen, US Welding) was 2.6 to 3.3 sLpm (STP, 273 K and 1 atm, L min^{-1}). The average linear flow velocity V_{ave} was 3 cm s^{-1} resulting in a Reynold's number R_e of ~80. The entrance length, the distance required for velocities to attain 95% of the laminar flow velocity profile from an initial plug flow profile,[16] is given by 0.1 $R_e a$ where a is the radius of the flow tube; it is ~15 cm. This indicates that a laminar flow profile was established before the kinetics were measured (measurements were not performed in the top 60 cm of the flow tube). See Appendix C for further justification of the assumptions of a laminar flow profile (also for the case where the gas flow was cooled to 287 K). The mixing time (the characteristic time to establish the diffusive profile of NH_3) is given by $a^2/5D_g$ where D_g is the gas-phase diffusion coefficient;[16] this time is ~5 s. In general, therefore, $[NH_3]$ was measured at distances between the detection region and the point of injection that were greater than (5 s) × (3 cm s^{-1}) = 15 cm.

NH_3 was taken from a dilute (27 parts per million by volume, ppmv) mixture in N_2. A small flow of this mixture (typically 1.5 sccm, STP cm^3 min^{-1}) was diluted and resulted in a flow of ~ 15 sccm N_2 containing ~ 0.4 ppmv NH_3 flowing through the injector. Further dilution of this flow by the main flow resulted in average $[NH_3]_0$ in the flow reactor that was typically 2 ppbv (parts per billion by volume), which is a number density of ~ 4×10^{10} cm^{-3}. The initial NH_3 mixing ratio for the mass accommodation coefficient measurements was varied over the range of 1−3 ppbv. It was as high as 12 ppbv in some experiments designed to test the effect of high $[NH_3]$.

Water vapor was entrained in a flow of N_2 by passing dry N_2 over liquid water that was gently heated. The liquid water contained ~0.5 wt % H_2SO_4 to suppress the elution of potential contaminant NH_3. The dew point of the flow reactor effluent was monitored with an EdgeTech dew point monitor (Dew Prime I, Milford Mass) after it had passed through a HEPA filter. The dew point monitor calibration was checked by condensing water vapor on the wall of the reactor that was held at 290 K. The reported dew point and the wall temperature agreed to better than 0.2 °C which results in an uncertainty in the partial pressure of H_2O, pH_2O, of ±1%. Relative humidity was varied from 8 to 91% resulting in particles with sulfuric acid content from 65 to 15 wt %,[21,24] respectively. At compositions of 25 and 50 wt % H_2SO_4, an uncertainty in pH_2O of 1% results in uncertainties in acid content of ±0.5 and ±0.2 wt %, respectively.

CIMS and Detection of NH_3. The effluent of the flow reactor passed through the chemical ionization region that was oriented transverse to the flow. The chemical ionization region (depicted in Figure 1) consists of an ion source, drift region (~2.7 cm long) and the inlet to the mass spectrometer. The ions were generated in an isolated source (0.6 mCi, ^{241}Am) and exited it via ~1 cm holes in two lenses that were separated by a 0.8 cm long static dissipative Teflon cylinder. These lenses were held at the same potential: applying an electric field between them significantly increased the total ion signal but increased even more the background ammonium ion signal (see below). Dry N_2 was flowed through the source at 40 sccm. The ions were brought through the transverse neutral flow in the drift region by applying an electric field of ~1100 V/cm (a potential difference of ~3 kV over the 2.7 cm distance between the exit of the source and the inlet of the MS). The inlet to the MS consisted of an inlet plate with a hole of ~1 mm diameter, an ion-drying region of ~0.5 cm in length that the ions enter in opposition to a flow of dry N_2 of ~30 sccm, and the inlet to the vacuum system (orifice diameter of 50 μm). An electric field of ~1100 V/cm in this region carried the ions to the ~50 μm orifice to the MS whereupon the ions were mass selected and detected.[17]

Ammonia was detected using proton transfer from H_2O−proton clusters:

$$NH_3 + H_3O^+(H_2O)_n \rightarrow NH_4^+(H_2O)_m + (n - m + 1)H_2O \quad (1)$$

The chemical ionization mass spectrometer (CIMS)[17] was set up for operation at ambient pressure (~610 Torr) resulting in a relatively weak E/N of ~ 5 Td (1 Td = 1 V/cm per 10^{17} molecule cm^{-3}). The calculated water proton cluster distribution peaks near $n = 5$ to 7 depending on pH_2O.[18] In eq 1, the precise values of m for a given n are not known. Viggiano et al.[19] measured a reaction rate coefficient k_1 for eq 1 of 2×10^{-9} cm^3 s^{-1} and reported that k_1 was not dependent on n up to $n = 8$.

The ion−molecule reaction time in the drift region for an ion with drift velocity v_d (equal to its mobility μ times the electric field) is given by

$$t_{ion} = 2.7/v_d = 2.7/(\mu 1100) \quad (2)$$

The mobility of an ion depends on its size and thus at first glance t_{ion} might be thought to depend on the number of water ligands on H_3O^+. In the current situation, however, the clusters are in rapid equilibrium (lifetime for decomposition of $H_3O^+(H_2O)_4$ is ~5 μs using the equilibrium constant at 300 K[18] and assuming a forward rate constant of 10^{-10} cm^3 s^{-1}; the larger clusters are even less stable) such that they drift at an overall rate that is a composite of the mobilities for the clusters. We assume a standard mobility (STP) of 2 cm^2 $(V\ s)^{-1}$, close to that of the $n = 3$ ion,[20] which results in a value for μ of 2.7 cm^2 $(V\ s)^{-1}$ at 610 Torr and 295 K. Thus the ion drift time is about 0.9 ms.

The concentration of ammonia, $[NH_3]$, is proportional to the quantity

$$[NH_3] \propto \ln\left(1 + \frac{\sum_m S\{NH_4^+(H_2O)_m\}}{\sum_n S\{H_3O^+(H_2O)_n\}}\right) \quad (3)$$

where S{ion} are the signals due to the ammonium and hydronium ions. The proportionality factor for eq 3 is $(k_1 t_{ion})^{-1}$ ≈ 6×10^{11} cm^{-3} for $k_1 = 2 \times 10^{-9}$ cm^3 s^{-1}.[19] The distributions detected by the MS changed somewhat with water partial pressure; however, for all conditions, 98% or more of the clusters $H_3O^+(H_2O)_n$ were contained between $n = 2$ and 6. The $NH_4^+(H_2O)_m$ ions were distributed over clusters with m between 1 and 5. Note that the measured distributions do not reflect the distributions in the ion drift region owing to some drying of

the ions in the inlet section. The sum of the ammonium cluster ions was typically a few percent or less of the total ions. Mass-dependent sampling, throughput, and detection efficiencies would affect the accuracy of eq 3. These effects would not significantly affect the results presented here because the ammonium cluster ions were a small fraction of the H_3O^+ ions.

A background level of ammonium ions was present that ranged between 0.2 and 0.5% of the total ions that were present. These ions appeared to be produced within the ion source as evidenced by their dependence on the source conditions. We did not identify the process but ammonium ions could arise from reactions of N^+ or N_2^+ ions clustering with water molecules (J. deGouw, private communication, 2001). This background was observed to depend on the pH_2O in the flow reactor. It was approximately 50% higher when pH_2O was increased to 10 Torr, and at 15 Torr H_2O it was about a factor of 2 larger than for dry conditions. The dependence on H_2O was significantly larger when the flow of dry N_2 through the source was decreased below 40 sccm suggesting that this background NH_4^+ signal may be related to diffusion of H_2O into the source. In the data analysis, the background ion signal was subtracted from the signal measured during the kinetics runs to obtain the first-order loss rate coefficient or it was included as a parameter in a weighted least-squares fitting routine using the function

$$f = S_0 \times e^{-k_z Z} + c \tag{4}$$

where S_0 is (would be) the signal ratio (lefthand side of eq 3) at zero interaction distance, k_z is the first-order loss rate coefficient (cm^{-1}), Z is the injector position, and c is the signal ratio due to the background signal.

A much smaller ammonia background signal eluting from surfaces (flow reactor wall and/or ion lenses) was noted after they had been exposed to NH_3. This increase in the NH_3 background signal was transient and was seen to diminish in time periods of an hour or so when exposure to NH_3 was stopped. A kinetics run was performed by initiating the recording of the signals when the injector was positioned to give a long exposure to the particles and then moving the injector in increments of 10−15 cm toward the ion source. The injector was then moved in increments back toward its original position (∼60 cm exposure) while recording the data and it was noted that data at long exposure (injector-to-ion region distances of 40 to 60 cm) was slightly higher at the end of a run than it was at the beginning. This increase was typically $(1-2) \times 10^{-4}$ in ion ratio which is equivalent to about 1×10^8 cm^{-3} of NH_3; the ratio was as high as 4×10^{-4} for a few measurements. This small increase in background signal is attributed to NH_3 desorbing from surfaces, especially those near to the detection region. Because data were recorded for large injector positions before and after these surfaces were exposed to high NH_3, and this small effect significantly affects the signal for only these data points, this effect is averaged out and is not expected to significantly impact the value of the extracted decay constant k_z.

This increase in the background signal is in the range of the expected partial pressure of NH_3, pNH_3, over $NH_3-H_2SO_4-H_2O$ solutions that contain roughly equal amounts of NH_3 and H_2SO_4. pNH_3 depends on the $NH_3-H_2SO_4$ ratio and also relative humidity. For relative humidities of 50−100%, the pNH_3 over a 1-to-1 $NH_3-H_2SO_4$ solution ranges from 10^{-12} to 10^{-11} atm ($0.3-3 \times 10^8$ cm^{-3}), respectively.[21] Thus, this small increase in NH_3 background signal could have been due to wall effects.

Particle Size and Concentration Measurements. Sulfuric acid particles were generated in a condensation-type particle generator where a flow of ∼80 sccm N_2 was passed over a small reservoir of hot liquid sulfuric acid (∼1 g, temperature of 110−150 °C); the $N_2 + H_2SO_4$ vapor was then cooled to room temperature.[14] This type of particle generator produces size distributions of particles that are well-described by a log-normal distribution[14] with a peak diameter (typically near ∼100 nm) that is controlled by the temperature of the liquid H_2SO_4. A portion (10−50%) of the 80 sccm flow of aerosol was mixed with the ∼3 sLpm main flow in a small tee (i.d. of ∼0.3 cm) where the main flow made a right-angle turn. In one test, large (∼0.25 μm diameter) particles in the flow tube were illuminated by a HeNe laser[1] and were observed to be uniformly distributed. It was concluded that there was good mixing of the small, particle-laden flow with the large main flow in the small tee.

Particle number densities, N_p, were measured with two different condensation nucleus counters (CNC, TSI Inc., St. Paul, MN, model numbers 3020 and 3760). The 3020 was used with a dilution of ∼20:1 to decrease the number density of $\sim 10^5$ cm^{-3} in the flow reactor to $\sim 5 \times 10^3$ cm^{-3} in the 3020. The dilution was accomplished by passing ∼5% of the flow required by the counter (230 sccm) through a small capillary[22] and the rest of the flow through a HEPA filter. Tests have confirmed that particle loss along the capillary is negligible.[22] The measurements conducted with the higher throughput CNC (TSI 3760) were performed with a dilution of about a factor of 10 and were corrected for coincidence (up to ∼10%). The dilution was accomplished by adding coaxially a dry, particle-free N_2 flow to the particle-laden flow from the reactor. Tests at low N_p confirmed that the dilution arrangement led to negligible particle loss. For measurements taken at a temperature T different than ∼296 K, N_p was multiplied by the ratio 296/T. During uptake measurements, the number densities of particles in the flow tube, N_p, ranged from 4×10^4 up to 1.5×10^5 particle cm^{-3}.

Particle size distributions were measured with a differential mobility analyzer (DMA). Particles were charged with a ^{85}Kr charger (TSI 3077). The N_2 sheath flow was 5.2 sLpm and it was humidified by diverting a portion of this flow through an H_2O reservoir followed by a HEPA filter. In some experiments the filter was not used (see Appendix) and thus a background [particle] was present in the DMA. The relative humidity of this flow was periodically checked with the dew point monitor during the measurements. The liquid water in this reservoir also contained a small amount of H_2SO_4 to decrease potential NH_3 contamination. An ultrafine condensation particle counter (based on the TSI 3025[1,23]) drawing 0.5 sLpm was used to detect the monodisperse aerosol exiting the DMA.

The log-normal distribution is given by

$$\frac{dN}{N_p} = \exp\left(-\frac{[\ln(D/D_p)]^2}{2[\ln \sigma]^2}\right)\frac{d \ln D}{\sqrt{2\pi}\ln \sigma} \tag{5}$$

The distributions obtained from the DMA were fit to eq 5 and the peak of the distribution, D_p, was typically 85 nm (varied from 70 to 170 nm) and the width of distribution, ln σ, was 0.28−0.30. As discussed in Appendix A, the surface area of the aerosol particles in the flow reactor was corrected for the known difference in acid content between that in the DMA and that in the flow reactor.[21,24] In the next paragraph we present the equations for calculating a reactant's first-order loss rate onto particles in an aerosol sample that is described by a log-normal distribution. A more detailed treatment is presented in refs 14,26.

Kinetics of Heterogeneous Reactions on Dispersed Particles. The gas-kinetic collision rate k_c of a reactant (of mean

thermal speed ω) with particles that have a log-normal distribution with radius r_p and width ln σ and a total number density N_p is given by

$$k_c = \frac{\omega}{4} SA_f N_p = \frac{\omega}{4} N_p 4\pi r_p^2 \exp(2(\ln \sigma)^2) \quad (6)$$

where SA_f is the surface area density in the flow reactor.[14,26] In the present experiments, k_c ranged from 0.15 to 1 s^{-1}. The existence of an efficient loss due to a surface (represented by γ, the gas−surface reaction probability) and gas-phase diffusion resistance can alter the true collision rate from that given by eq 6. These processes can be taken into account using the Fuchs-Sutugin expression.[25] For a particle of radius r, the first-order loss rate k_m for a species with an uptake coefficient γ is given by[25,26]

$$k_m = \gamma k_c (1 + \gamma\lambda(r))^{-1}, \quad \lambda(r) = \frac{0.75 + 0.283K_n}{K_n(1 + K_n)}, \quad K_n = \frac{3D_g}{\omega r} \quad (7)$$

where K_n is the Knudsen number, and D_g is the gas-phase diffusion coefficient for the reactant ($cm^2\ s^{-1}$). This expression can be applied to a dispersed aerosol sample by integrating it over the particle size distribution.[14,26] If the particle size distribution is log-normal, there is an alternate analysis procedure. The so-called "surface-area weighted radius" $\bar{r}_s$ (the ratio of the third moment of the distribution to the second moment of the distribution) is substituted for r in the expression for the Knudsen number.

$$\bar{r}_s = r_p \exp(2.5(\ln \sigma)^2), \quad \bar{K}_n = \frac{3D_g}{\omega \bar{r}_s}$$

$$\lambda(\bar{r}_s) = \frac{0.75 + 0.283\bar{K}_n}{\bar{K}_n(1 + \bar{K}_n)} \quad (8)$$

For the particle distributions here (ln $\sigma \sim 0.3$ and $\bar{r}_s \leq 90$ nm) this alternate analysis procedure is accurate to better than 1% in comparison to numerical solutions of the integral presented in ref 26. In the present experiments, $\lambda(\bar{r}_s)$ is 0.1−0.25; thus the maximum uptake rates are 10−25% less than the gas-kinetic rates given by eq 6 for a unit uptake probability ($\gamma = 1$).

Effect of NH_3 Uptake on Sulfuric Acid Particles. We assume that the particle size was not significantly altered by the uptake of NH_3 for the low levels of NH_3 employed in the uptake experiments (1.5 to 3 ppbv). This is backed up by measurements of the particle size distributions before and after exposure to ~2 ppbv NH_3 where it was found that the measured particle size distribution did not change.

A typical value for the final ammonium-to-sulfuric acid ratio in the particles can be estimated by assuming all the NH_3 is taken up by the particles. For $N_p = 10^5\ cm^{-3}$, $r_p = 0.050\ \mu m$, ln $\sigma = 0.3$, and 40 wt % sulfuric acid particles, the number of H_2SO_4 molecules in the particles per unit volume is $\sim 4 \times 10^{11}\ cm^{-3}$. Initial [$NH_3$] is generally $4 \times 10^{10}\ cm^{-3}$, so the final $NH_3-H_2SO_4$ ratio is typically ~0.1. See Appendix A for results from measurements with high levels of NH_3 present where this ratio was ~1.

NH_3 that is taken up diffuses throughout these small particles very rapidly. An approximate time scale for diffusion of a species with diffusion coefficient D_l in a particle of radius a is given by a^2/D_l. For $a \sim 100$ nm and $D_l \sim 10^{-6}\ cm^2\ s^{-1}$, this time is $\sim 10^{-4}$ s.

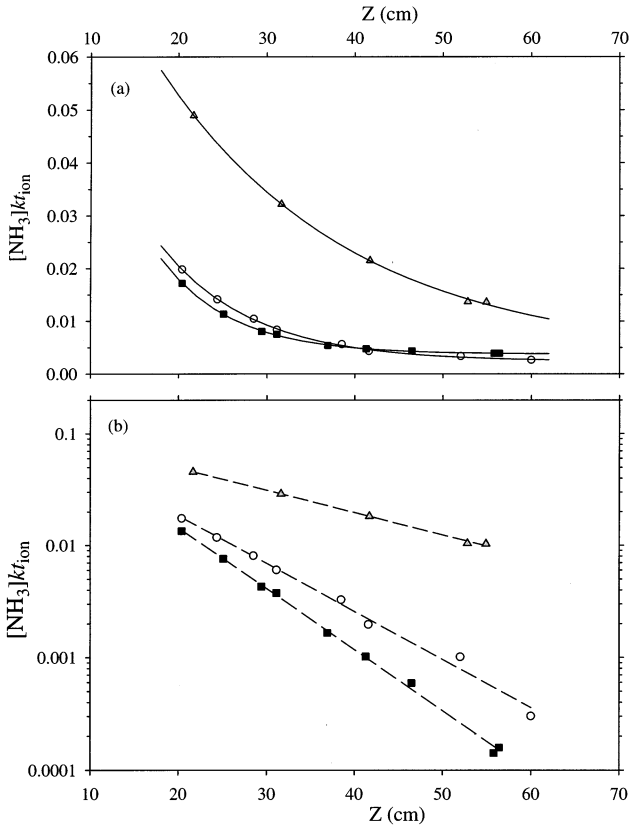

Figure 2. Signal due to NH_3 (a, linear scale; b, logarithmic scale with background signal subtracted) plotted versus injector position. NH_3 loss to the wall at 295 K in the absence of particles is shown as triangles. Shown as circles and squares is the NH_3 signal in the presence of 52 and 22 wt % H_2SO_4 particles, respectively. Experimental conditions and log-normal parameters (X wt %: {pH_2O, T, N_p, D_p, log σ}) for the two experiments are 52 wt %: {5.8 Torr, 295 K, $6.6 \times 10^4\ cm^{-3}$, 85 nm, 0.127} and 22 wt %: {11.5 Torr, 289 K, $5.9 \times 10^4\ cm^{-3}$, 118 nm, 0.132}.

Results and Analysis

Typical kinetic data are shown in Figure 2, a plot of [NH_3]kt vs injector position for loss of NH_3 onto the reactor wall only (triangles) and for the loss of NH_3 onto particles composed of 52 and 22 wt % H_2SO_4 (circles and squares, respectively). Figure 2a shows the data on a linear plot along with lines from least-squares fits of the data to eq 4. Figure 2b shows the same data plotted on a logarithmic scale with the background c subtracted from the data. It is apparent from these plots that the loss of NH_3 is characteristic of a first-order process.

The extraction of the NH_3 mass accommodation coefficient α from the measurements is as follows.[14] The first-order loss rate coefficient k_z (cm^{-1}) was obtained from the slope of a plot such as Figure 2b or from eq 4 using a weighted least-squares fitting procedure. Multiplying this value by the average flow velocity results in a plug-flow first-order loss rate coefficient (s^{-1}) k_{plug}. The measured first-order loss rate coefficient that is due to uptake onto particles, k_m, is calculated from k_{plug} and the observed wall loss rate coefficient k_w (typically 0.15 s^{-1}) according to eq 9:

$$k_m = (k_{plug} - k_w) \times 1.61 \times \left(1 + \frac{k_z D_g}{V_{ave}}\right) \quad (9)$$

This equation takes into account the laminar flow velocity profile and gas-phase diffusion within the cylindrical reactor.[27,28] The last factor in eq 9 can be attributed to axial diffusion within the flow reactor[28] and is a maximum of 2% for the results presented here. The accuracy of eq 9, determined by comparison to the Brown calculation,[27] is better than 1.5% over the range of conditions of the present work. Division of k_m by the first-order collision rate of NH_3 with particles k_c yields a value for the extracted reaction probability, γ_{ex}. The diffusion resistance is then taken into account according to the equations presented above resulting in γ, the measured reaction probability

$$\gamma_{ex} = \frac{k_m}{k_c}, \quad \frac{1}{\gamma} = \frac{1}{\gamma_{ex}} - \lambda(\bar{r_s}) \tag{10}$$

As mentioned above, this latter correction amounts to 10−25% when γ_{ex} is close to unity. Here, because there is no significant desorption of NH_3 from the particles (as discussed above the saturated pNH_3 over ammonium bisulfate solutions is <0.01 ppbv[21]), the observed γ is taken to be the mass accommodation coefficient α.

As opposed to the rate of loss on the particles, gas-phase diffusion is the controlling factor for the loss of NH_3 onto the reactor walls. The first-order wall loss rate coefficient, $k_{d.l.}$, in a cylindrical flow reactor for a species that is efficiently lost on the wall in the absence of particles is given by $3.65D_c/a^2$ where D_c is the diffusion coefficient and a is the reactor diameter.[27,28] The average of the first-order wall loss rate coefficients k_w (equal to the experimental k_z in the absence of particles times V_{ave}) measured at 296 K was 0.15 s^{-1} which results in a D_c of 0.275 cm^2/s at $pN_2 = 610$ Torr or a value of 0.220 (±7%) atm cm^2 s^{-1} for the pressure-independent diffusion coefficient for NH_3 in N_2. This value compares favorably with previously reported values for pD_c of 0.241 atm cm^2/s at 293 K[44] and, for NH_3 in air, of 0.227 and 0.234 atm cm^2/s at 293 and 298 K, respectively.[45]

The uncertainty in the measured mass accommodation coefficients is typically ±20−25% (combined precision and accuracy). Precision errors are due to uncertainties in the measured loss rate coefficient (±8−15%) and surface area (±7−9%). The uncertainty in k_m is mainly due to the determination of k_z to ±5% which results in a ±7−15% uncertainty in the quantity $k_{plug} - k_w$. Uncertainties in V_{ave}, ±3%, and in eq 9, 1.5%, and eq 10, ±2%, are minor sources of error. The surface area uncertainty is due to the uncertainty in the size of the distribution (±2.5% in D_p is ±5% in SA_f) and the random uncertainty in N_p due to the uncertainty in the dilution factors (±5% for measurements with the 3760 and ±7% for those with the 3020). In addition, an uncertainty was included that scales linearly with the calculated increase in the size of particles, eq 11, i.e., swelling of the particles when the flow reactor was cooled to a temperature lower than that of the DMA. The latter uncertainty was assigned a value of ±10% for a factor of 2 swelling based on a potential 0.2 K temperature uncertainty. Finally, we add in an additional accuracy uncertainty of ±10% to account for uncertainties in determining the absolute N_p. This was determined by comparing the N_p reported by the two counters that were sampling the same flow of aerosol. They generally agreed to within ±5% but sometimes this comparison resulted in discrepancies of 10%.

Figure 3 is a plot of the measured mass accommodation coefficients versus H_2SO_4 content. The error bars in this plot do not contain the accuracy error of ±10% in N_p because this uncertainty is not dependent on acid content (both counters were employed over the entire range of H_2SO_4 content). The main point of Figure 3 is to show the lack of any variation of α with acid content with an uncertainty dictated by the precision uncertainties. Measurements taken at temperatures of 293−296.5 K are presented as filled circles while measurements at 287−292 K are presented as open circles.

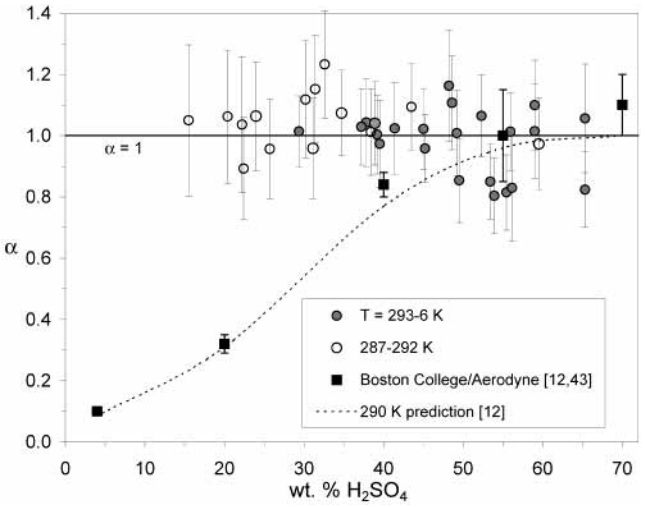

Figure 3. The measured mass accommodation coefficients for NH_3 plotted versus H_2SO_4 content. Filled symbols are results from measurements near room temperature (293 to 296.5 K) and open symbols are from experiments at temperatures between 287 and 292 K. Previous data at 20, 40, 55, and 70 wt % are from Swartz et al.[12] and that for ~4 wt % is that of Shi et al.[43] The dashed curve is a prediction for α deduced from the measurements reported by Swartz et al.[12] for a temperature of 290 K.

The most recent measurements of α[12,43] are shown as filled squares along with a curved line from an equation presented by Swartz et al.[12] that was deduced from their measurements of α as a function of acid content and temperature. While good agreement is exhibited for the more concentrated solutions, it is apparent that there is serious disagreement between these two sets of data for acid contents < 40 wt % H_2SO_4. Earlier researchers[7−11] report the efficiency of NH_3 uptake from 0.1 to 1 over a wide range of sulfuric acid contents. As pointed out by Swartz et al.,[12] these early measurements were probably affected by a relatively high NH_3 content of the particles. The rate of uptake of NH_3 in these experiments was generally inferred from the extent of neutralization of the H_2SO_4 particles and this was carried out to an overall ammonia content that corresponded to NH_4HSO_4 or higher. Therefore, those uptake efficiencies probably do not correspond to the value of α for uptake onto nearly NH_3-free sulfuric acid solutions.

Discussion

There is a substantial discrepancy between the dependence of α_{NH_3} on acid-content reported here and that reported by Swartz et al.[12] The average of the present data for sulfuric acid content of 40 wt % and greater is 0.98 (±0.05, 95% confidence level) and that for H_2SO_4 content < 40 wt % is 1.04 (±0.04). The total uncertainty can be obtained by adding the systematic uncertainty in N_p of ±10% yielding $\alpha_{NH_3} = 0.98 \pm 0.15$ and 1.04 ± 0.14 for 40−65 and 15−40 wt % H_2SO_4, respectively. The agreement with the Swartz et al. data for H_2SO_4 content > 40 wt % is good but for the dilute solutions at high pH_2O it is not. Their data suggest that α should decrease markedly when the H_2SO_4 content is less than 40 wt %. If our measurements are an accurate representation of the mass accommodation process for NH_3 onto dilute H_2SO_4 solutions then this disagreement has several, significant ramifications.

For one, the neutralization rate of dilute sulfuric acid particles in the atmosphere can be up to 5 times faster than the Swartz et al.[12] data suggests. The gas-phase NH_3 loss rates accompanying this process can be much faster than the low values reported for α would suggest. This will impact most our understanding of the formation and growth of small ($a \leq 100$ nm) particles and thus how these particles might influence chemical and climate processes. Furthermore, very small particles (a few nanometers in diameter) containing H_2SO_4 will be stabilized more efficiently than the Swartz et al.[12] data suggests. Assuming that α_{NH_3} measured on 100 nm droplets applies to 5−10 nm sized sulfuric acid droplets, the stabilization and growth of these small particles by addition of NH_3 will be rapid no matter what their composition. Note that a rapid neutralization of concentrated sulfuric acid particles (i.e., a relative humidity of ∼10%) is consistent with kinetic considerations applied to the observation[2] of very small $NH_3-H_2SO_4$ clusters (∼1 nm diameter). At the low levels of NH_3 [200 pptv] and short interactions times (∼4 s) employed in that study, these small clusters could not have been observed unless NH_3 uptake was efficient.

Second, the discrepancy in the α_{NH_3} shown here highlights a potential problem in the analysis of the results of droplet train experiments operated at high pH_2O. Swartz et al.[12] presented measurements of the uptake of NH_3 onto sulfuric acid particles over a wide range of conditions and used the results to provide additional validation of their treatment of gas-phase diffusion.[29] If the physical interaction we purport to study (i.e., mass accommodation) pertains to their experimental conditions, then some aspect of their analytical approach might be flawed. This may have quite far-reaching implications as it calls into question the reported accuracy of the mass accommodation coefficient measured under these conditions (i.e., measurements near room-temperature involving dilute aqueous solutions).

It should be mentioned that the droplet train technique has been successfully used to study and understand a wide variety of atmospheric heterogeneous processes. The discrepancy in α_{NH_3} reported here indicates that, if there is a problem with the droplet train results, it arises for results only from experiments conducted at relatively high H_2O partial pressures. For the typical particle size in the droplet train apparatus, a high pH_2O gives a relatively low Knudsen number, ∼0.1, while the lower pH_2O over concentrated H_2SO_4 solutions gives $K_n \sim 1$, close to the experimental K_n of 2-to-3 of this work, which does not depend on pH_2O. If the discrepancy reported here is due to an error in their results, it is in the interpretation of their data at low Knudsen number and/or high pH_2O.

There are a few measurements of the mass accommodation coefficient for other species that are not in accord with those presented by Davidovits, Kolb, and Worsnop of the Boston College−Aerodyne Inc. (BCA) collaboration. These come from studies of the interactions of the strong acids HCl and HNO_3 with aqueous surfaces. These types of interactions are expected to be strong and their incorporation into the bulk of a liquid would be facile. The BCA analysis of their results from experiments performed near room temperature suggest that α is ∼0.05−0.1 for both HCl and HNO_3 uptake onto water and/or dilute sulfuric acid solutions.[32−34] As the temperature is decreased to 273 K, α increases to ∼0.2. These values for α are remarkably low and indicate that the interactions of HCl and HNO_3 with aqueous surfaces are not facile near room temperature.

However, a different measurement of α for HCl suggests otherwise. Hanson and Lovejoy[36] measured the reaction probabilities of HCl onto 26 and 34 wt % H_2SO_4 at ∼274 K and reported values for α_{HCl} of 0.8 (±0.2) and 1.0 (±0.5), respectively. After that study was published, the BCA collaboration published a reinvestigation of HCl uptake onto sulfuric acid (Robinson et al.[35]). They reported additional measurements of α_{HCl} that bolster their earlier measurements, suggesting that α_{HCl} for these conditions indeed has a value of 0.2 ± 0.05. The source of this clearly important discrepancy was not investigated in either of these articles.

A recent study on the growth of HNO_3-H_2O liquid droplets at 278 K in an expansion chamber[37] showed that droplet growth was consistent with values of unity for both α_{H_2O} and α_{HNO_3} at 100% relative humidity (i.e., appropriate for liquid water). The BCA collaboration[32,34,38] report measurements of α_{HNO_3} and α_{H_2O} for uptake onto pure water at temperatures near 278 K. Their values are ∼0.16 and 0.2 (with reported uncertainties of ∼±20%) for HNO_3 and H_2O, respectively. Rudolf et al.[37] more confidently state that α_{HNO_3} is unity at relative humidities of 60 and 70% at 278 K; their data are inconsistent with a value for α_{HNO_3} as low as even 0.3 for uptake onto dilute HNO_3 aqueous solutions. In the BCA view of incorporation of a gas molecule into a bulk liquid,[33,34] the mass accommodation coefficient does not depend on H_2SO_4 content (up to ∼40 wt %) for the uptake of HNO_3 and HCl. If α is also independent of HNO_3-content, a reasonable assumption, then a substantive discrepancy exists here also.

Molecular dynamics simulations of the interaction of ethanol with a water surface and the bulk liquid show no significant barrier for entry of an ethanol molecule into the bulk water.[39,40] Wilson and Pohorille[39] further state that their simulations show that the mass accommodation coefficient is 0.98. The BCA collaboration report measurements that indicate that α for ethanol on pure water is ∼0.04.[41]

With the exception of the NH_3 results, the discrepancies noted above involve the comparison of results from chemical or physical systems that may be quite different. Further consideration of these differences might lead to the alleviation of some of the discrepancies. The presently noted discrepancy in α_{NH_3} is more troubling, however, because the two different experimental techniques investigated similar chemical interactions. Yet a common element in all the discrepancies is that the results from the droplet train apparatus were derived from experiments conducted at relatively high pH_2O (low K_n). If the discrepancy in α_{NH_3} is traced to the droplet train results, a reevaluation of the droplet train experimental results for other chemical systems at high pH_2O should also be considered.

There are a few potential sources for the discrepancy in α_{NH_3} that might be significant. Swartz et al. exposed sulfuric acid particles to NH_3 at levels that were about 1000 times the $[NH_3]$ of the present study. This would lead to fluxes of ammonia that were 1000 times greater than those of the present study. In a companion paper[43] BCA presented a numerical calculation of diffusion within the liquid that shows the NH_3 fluxes they used should not affect the measurement of α_{NH_3}. Nonetheless, the widely different NH_3 fluxes in the two experiments might play some role in the discrepancy. This difference between the experiments is specific to the NH_3-sulfuric acid system. The next two potential difficulties are specific to measurements that are performed at high pH_2O.

A potential impediment to uptake is the existence of a net flux of H_2O vapor away from the droplet. Although a net H_2O flux was considered in ref 29c, it does not seem to have been fully explored for the droplet train apparatus. There are temperature gradients near the surface of the liquid in the droplet train experiment;[29a] apparently it is common that the interior

of a droplet is slightly warmer than its surface. Rates of diffusion can be significantly impeded even for slight temperature imbalances: a 0.2 K deviation would lead to a net flux of H_2O from the surface that is equivalent to 1% of the gross flux of H_2O. See Appendix B for an estimate of the effect on the uptake of an absorbent if there is a significant flux of water vapor from (or onto) the droplet surface.

Gas-Phase Diffusion Considerations. As mentioned above, the K_n in the present experiments is $\sim$ 2 to 3 and is nearly independent of pH_2O. Therefore, the diffusion correction (eqs 7,8) is nearly independent of pH_2O. K_n for the experiments of Swartz et al. is in this range for experiments at low pH_2O; however; it can take a maximum value of only $\sim$0.3 when pH_2O is $\sim$10 Torr, i.e., for the most dilute sulfuric acid solution they studied. Therefore, the effects of gas-phase diffusion have an H_2SO_4-content dependency via the Knudsen number dependency in their experiment. A changing rate of diffusion with pH_2O that is not fully taken into account is a potential candidate for the discrepancy in the NH_3 results.

There is a large base of empirical evidence that corroborates the treatment of diffusion in the droplet train apparatus,[29b] yet this corroboration lacks independent verification. It can therefore be argued that gas-phase diffusion to a droplet train is not yet well understood. Furthermore, because the correction due to diffusion can have considerable leverage on the value of the extracted uptake coefficient (e.g., when K_n is $\ll 1$ in eq 7), very high uncertainties can be introduced when gas-phase diffusion significantly limits the measured uptake. Their analysis of diffusion leads to relatively small corrections to the measured loss rates even at high pH_2O. The relatively small corrections led them also to assign relatively small uncertainties. However, if the correction for diffusion were to be increased, the uncertainty of the resulting γ would also increase. Therefore, a second effect of a potential underestimate of the effects of diffusion is an assignment of an uncertainty that is too low. This might also contribute to the discrepancy in α_{NH_3} noted here.

For the droplet train results, an alternative analytical procedure can provide a measure of the uncertainty in the rates of diffusion to a droplet train. For example, the use of the real droplet size in the diffusion expression (eq 7) rather than an effective droplet size might yield a representative range of the uncertainty. This exercise for their results for H_2O_2 at 274 K[29a] results in a value for α of 0.5 for a droplet size of 150 μm, whereas the value reported was $\sim$0.2. Note that the pD_g for H_2O_2 in H_2O and in Ar reported in ref 29a are not in accord with the Chapman-Enskog procedure[52] using suitable molecular parameters. They take values of $\sim$0.11 atm cm^2/s at 274 K as opposed to the 274 K values in ref 29a of $\sim$0.21 atm cm^2/s. The variation in extracted α from their reported value of 0.2 to the alternate calculation of 0.5 might be an indication of the precision of the measurement technique under these conditions.

Recently, a fluid dynamics simulation[42] has been published that provides a basis for evaluating diffusion in the droplet train apparatus. Their results indicate that the BCA method for treating their data, although qualitatively correct, can result in an uncertain value for the mass accommodation coefficient. Their most significant finding is that the BCA treatment resulted in a value for α (0.35) that is substantially lower than what was used as an input in the model ($\alpha = 1$). When the droplets are closely spaced, the concentration of the absorbent at the droplet surface is less than that calculated by considering the rate of diffusion to a single, isolated droplet (e.g., eq 7).

The experimentally measured loss rate is proportional to the quantity $\gamma_{ex} n_{ave}$ where n_{ave} is the average absorbent concentration while the loss is actually due to uptake on the surface which is proportional to the quantity γn_s where n_s is the absorbent concentration at the surface of the droplet. To obtain the true uptake coefficient γ (or α) from the measured value γ_{ex}, a value for n_s/n_{ave} must be accurately calculated. Morita and co-workers showed that the current treatment does not give an accurate value for this ratio and thus the resulting γ is not quantitatively correct at low K_n. They also found that the calculation of the diffusion correction using the actual droplet diameter in eq 7 is not quantitatively correct.

Conclusions

The present measurements show that the mass accommodation coefficient of NH_3 onto sulfuric acid droplets is essentially unity for a wide range of compositions. The average value for α_{NH_3} over the entire range of conditions examined here is 1.01-($\pm$0.14). This is in accord with expectations when considering the uptake of a strong base by an acid solution. It is not in accord with recently reported results using a droplet train apparatus.

The successful use of the droplet train apparatus in the study of heterogeneous chemistry is an impressive technological achievement. There are many important results and discoveries that have been made using this technique. A number of different groups have adopted it for use in the study of atmospheric heterogeneous chemistry, e.g., refs 30,31. However, the currently accepted procedure of calculating the mass accommodation coefficient from results obtained with the droplet train apparatus might have to be revised at high pH_2O. It is reasonable to suppose that the influence of gas-phase diffusion in a droplet train apparatus could be better understood. If there is a net evaporation of water vapor from the droplets this might also significantly impede the rate of uptake. We believe this improved treatment and consideration of other effects might lead to an increase in the uncertainty of the extracted γ as well.

If significant revision of the droplet train data at high pH_2O is necessary, it might lead to the result that the data is consistent with an α equal to unity for many molecules. We have shown in this work that this might be the case for α_{NH_3}; results from similar experiments on HCl suggest that this might also be the case for α_{HCl}.[36] Indeed, it might lead to the general result that many mass accommodation coefficients are not dependent on temperature. The truth of this speculation awaits further independent experimental study of the chemical systems that BCA has reported on. Furthermore, if these assertions hold up under scrutiny, the quasi-nucleation model for α developed by BCA[46] may not have a wide scope of applicability.

Acknowledgment. We thank P. McMurry for the use of the ultrafine particle CNC and F. Eisele for use of the 3020 CNC. Comments on the text by J. Orlando and J. Greenberg and the anonymous reviewers were very helpful in improving the manuscript. Conversations with E. R. Lovejoy, A. Morita, and G. Nathanson are gratefully acknowledged. Comments on this manuscript from BCA provided by P. Davidovits were also appreciated.

Appendices

Appendix A. Considerations in Determining the Size Distributions. The H_2SO_4 content of an $H_2SO_4-H_2O$ solution is determined by temperature and the measured water partial pressure.[21,24] This is the composition a particle will attain if it is of sufficient size so as to not be affected by the Kelvin effect (certainly true here). The flow reactor conditions were not always precisely met by the conditions in the DMA, thus the particle distribution in the flow reactor was at times different

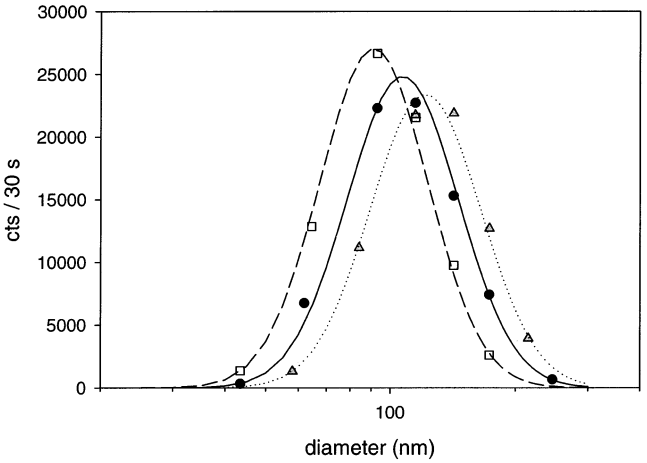

Figure A1. Three size distributions are shown for H_2SO_4 particles that were exposed to varying amounts of H_2O in the sheath flow for the DMA. Squares are conditions such that the particles were composed of 74 wt % H_2SO_4, circles are for conditions in the DMA sheath flow that matched those of the aerosol in flow (56 wt % H_2SO_4), and triangles are for conditions such that the particles were composed of 40 wt. % H_2SO_4. The fitted log-normal distributions are shown as the curves for each case. The particles swelled as expected (surface area was within 5%) according to eq 10.

from that measured with the DMA. The H_2SO_4 content of the particles in the flow reactor was varied by changing pH_2O (from 3 to 15 Torr) at a constant temperature or by changing temperature (from 296 to 287 K) at a constant pH_2O. In the former method, the relative humidity in the DMA was changed along with that in the flow reactor, thus the size distribution measured with the DMA was very close to that present in the flow reactor. In the latter method the DMA was not cooled along with the reactor, thus the particles lost a significant amount of H_2O during their transit from the cooled flow reactor to the warm DMA. For both methods, the particle size distribution present in the flow reactor was calculated from the measured distribution, temperatures, and pH_2O according to the thermodynamics of $H_2SO_4-H_2O$ solutions.[21,24,47] Thus the surface area density in the flow reactor, SA_f, is related to that given by the DMA, SA_{DMA} via

$$\left(\frac{SA_f}{SA_{DMA}}\right) = \left(\frac{r_f}{r_{DMA}}\right)^2 = \left(\frac{[H_2SO_4]_{DMA}\rho_{DMA}}{[H_2SO_4]_f\rho_f}\right)^{2/3} \qquad (11)$$

where ρ_X indicates the density of H_2SO_4/H_2O solutions[47] in region X. This procedure resulted in ratios for SA_f/SA_{DMA} that were generally close to unity (within 5%) for the measurements where pH_2O was varied and the flow reactor was at 294 K or higher. This ratio was in the range 1.1−1.2 for the measurements where the flow reactor was cooled to temperatures of 295 to 292 K. This ratio ranged as high as a factor of 2.3 when the flow reactor was cooled to 287 K. Fried et al.[22] report on experiments that confirm the swelling of particles according to eq 11. Shown in Figure A1 are distributions of particles with different amounts of water vapor added to the sheath flow of the DMA such that the particles contained 74, 56, and 40 wt % H_2SO_4. The increase in the size distribution is matched well by that predicted (predicted surface area from eq 11 is within 5% of the observed surface area increase). Finally, the resulting reaction probabilities did not depend on which method was used.

Sizing an aerosol particle with a differential mobility analyzer is a technique that is generally accepted as quite accurate ($\Delta D_p \sim 2\%$). Special considerations arise in the application of this technique in the present experiment.

The aerosol particles used in the experiments were not monodispersed, thus evaluating the amount of doubly charged particles in the measured distribution is not straightforward. For number densities of particles on the order of 10^5 cm^{-3}, the type of ^{85}Kr charger used here does not bring the charge distribution of the particles to the equilibrium charge distribution, even when it is fresh.[48] The ^{85}Kr charger used in the experiments here was ~15 years old and thus its strength is likely to be much less than the original 2 mCi. Therefore, the amount of double-charging here will be much less than is given by the equilibrium Boltzman distribution. For a significant fraction of the experiments, the particles were small enough (D_p < 90 nm) and numerous enough (~10^5 cm^{-3}) that double charging of particles was negligible. This is seen in Figure A1 that shows measurements of typical distributions that are well described by log-normal distributions.

The amount of double charging that a particle obtains depends strongly on its size. An experiment was performed where the aerosol particle size in the ^{85}Kr charger was increased by humidifying this flow so that the particles contained ~18 wt % H_2SO_4. This was accomplished by passing the aerosol through a conditioner that contained a bulk 18 wt % H_2SO_4 solution while holding the DMA sheath relative humidity at ~10%. The measured distributions with and without the conditioner (particles contained ~70 or ~18 wt % H_2SO_4 in the charger and thus had D_p of ~80 and ~140 nm) were nearly identical, indicating that double charging is not significant.

The humidified sheath flow for the DMA was checked for NH_3 by introducing it into the ionization region where it was found that pNH_3 was negligibly low. However, high levels (2−20 ppbv) of an amine with formula $C_6H_{13}N$ were observed. This was traced to the HEPA filter on the exit of the water source. Measured particle distributions without the filter were no different than those with the filter inline (except for a background count rate on the monodisperse outlet of 5−20 Hz due to particles produced in the humidifier).

Effect of NH_3 When NH_3 Is Comparable to H_2SO_4. In one set of measurements, [NH_3] was raised to ~12 ppbv and the observed particle size distribution was observed to shrink: D_p decreased by about 7%. Also, the width of the distribution increased, indicating that the large particles did not shrink as much as the small particles did. This amount of NH_3 (2.3×10^{11} cm^{-3}) is comparable to the amount of H_2SO_4 that was present in the particles (1.7×10^{11} cm^{-3}), thus some portion of the particles may have approached the composition of ammonium bisulfate (NH_4HSO_4). At this relative humidity, 35%, a decrease in diameter of ~13% for a $H_2SO_4-H_2O$ particle is expected upon absorption of one NH_3 molecule for every H_2SO_4 molecule. This size change was based on a constant amount of H_2SO_4 in the particle and assuming the particle remains liquid (35% RH is well above the efflorescence point, the RH below which crystallization occurs, 22%[49]) along with the densities and water activities of $NH_4HSO_4-H_2O$[49] and $H_2SO_4-H_2O$[21,24,47] solutions. The kinetic data for NH_3 uptake in this experiment resulted in an uptake coefficient that was ~0.5—a value much smaller than that for measurements when NH_3 was low.

Appendix B. Flux of Water Vapor from the Surface. A rough estimate of the flux $J_{\Delta F_{H2O}}$ of the absorbing molecule that is carried from the surface due to a net flux of water vapor from the surface ΔF_{H_2O} can be calculated by

$$J_{\Delta F_{H_2O}} = n_s V_{\Delta F_{H_2O}},\ V_{\Delta F_{H_2O}} = \frac{\Delta F_{H_2O}}{n_T} \qquad (12)$$

where n_s is the number density of the absorbing molecule near the droplet surface, $V_{\Delta FH_2O}$ and n_T are the net velocity and total number density of the carrier gas + H_2O vapor, evaluated near the surface of the droplet. As an example, we will assume a 0.25% net flux from a droplet at 292 K, which yields a flux of water vapor away from the droplets of $\Delta F_{H_2O} = 2 \times 10^{19}$ molecule cm^{-2} s^{-1}. Due to gas-phase diffusion, n_s near the surface is less than that far from the surface, n_∞, let us assume $n_s = 0.75 \times n_\infty$. This small concentration gradient is the expected one if there is a relatively small correction (~33%) for diffusion (i.e., this gradient is in accord with the BCA treatment of diffusion at high pH_2O). With $n_T = 8 \times 10^{17}$ cm^{-3}, the magnitude of the flux given by eq 12 is 20(cm/s) $\times$ n_∞.

The flux of absorbent molecules toward the droplet surface due to diffusion is given by Fick's law, $J_{diff}(a) = -D_g \nabla n(r)|_{r=a}$. With $n(r) = n_\infty - (n_\infty - n_s)(a/r)$,[51] the gradient evaluated at the surface $\nabla n(r)|_{r=a} = (n_\infty - n_s)/a$. For $D_g = 7$ cm^2/s which is appropriate for NH_3 diffusion at a total pressure of ~22 Torr (of which $pH_2O = 16$ Torr) we get that $J_{diff}(a) = -D_g(n_\infty - n_s)/a = -7(cm^2/s) \times 0.25 n_\infty/0.0100$ cm $= -175$ (cm/s) $\times$ n_∞. For this example then, the overall flux is reduced from the unimpeded diffusive flux by 11%.

The flux of H_2O molecules ΔF_{H_2O} used in this example requires a heat transport from the interior of the droplet to its surface of ~0.0015 J/s, which is at the low end of the range of fluxes calculated in Worsnop et al.[29a] Furthermore, this ΔF_{H_2O} emanating from droplets of $a = 100$ μm that are spaced apart by 1500 μm in a 10 cm length leads to a net flow of water vapor of 0.06 STP cm^3 s^{-1}. This is only about 1% of the total flow in the droplet train apparatus and it is possible that this amount of flow exiting the droplet train apparatus through the droplet entrance or exit is not easily noticed. It is also possible that a portion of this excess H_2O flow can recondense on droplets that are slightly cooler and are outside the region where the kinetics are measured. If this occurs to a significant extent, then a larger ΔF_{H_2O} could be supported and the impediment to the uptake of the absorbent would be even greater than for the example quoted above. This flux also leads to an amount of water lost (in a droplet transit time of 0.01 s) of about 200 monolayers which is equivalent to a negligible change in the radius of the droplet (0.06 μm).

The flux from eq 12 does not include any absorbent molecules on the surface that might be carried off during the evaporation process. This might be especially important for molecules that have a large surface excess Gibbs free energy (i.e., a much larger mixing ratio in the surface layer than in the bulk).

The flux ΔF_{H_2O} might also cause gradients in the concentration of CH_4, which is present as a tracer and assumed to be uniformly distributed throughout the reactor. This may then cause an error in the loss rate measurement of the absorbent as it is normalized to the loss for CH_4. Note that in the transverse droplet train apparatus there was a net loss of CH_4 upon droplet switching when the flow tube pressure was supposed to perfectly balanced.[29a] It is not clear what that observation implies for $J_{\Delta F_{H_2O}}$ nor what it means for the pressure balance in the primary setup of the experiment where the droplet train is aligned along the central axis of the cylindrical flow tube.

It is important to understand this effect for making a proper estimate of its impact on the results. Its magnitude and sign are likely to depend in a complicated manner on droplet size, the difference between the initial and final temperatures of the liquid, and pH_2O. In addition, the rates of diffusion are very important in this context. For example, using the results of Morita et al.,[42] n_s is likely to be much less than 0.75 $\times$ n_∞, which will decrease the impact of this effect. Although it is not entirely clear from the discussion in Worsnop et al.,[29a] it appears that they believe there is a net evaporation rather than a net condensation in their experiments.

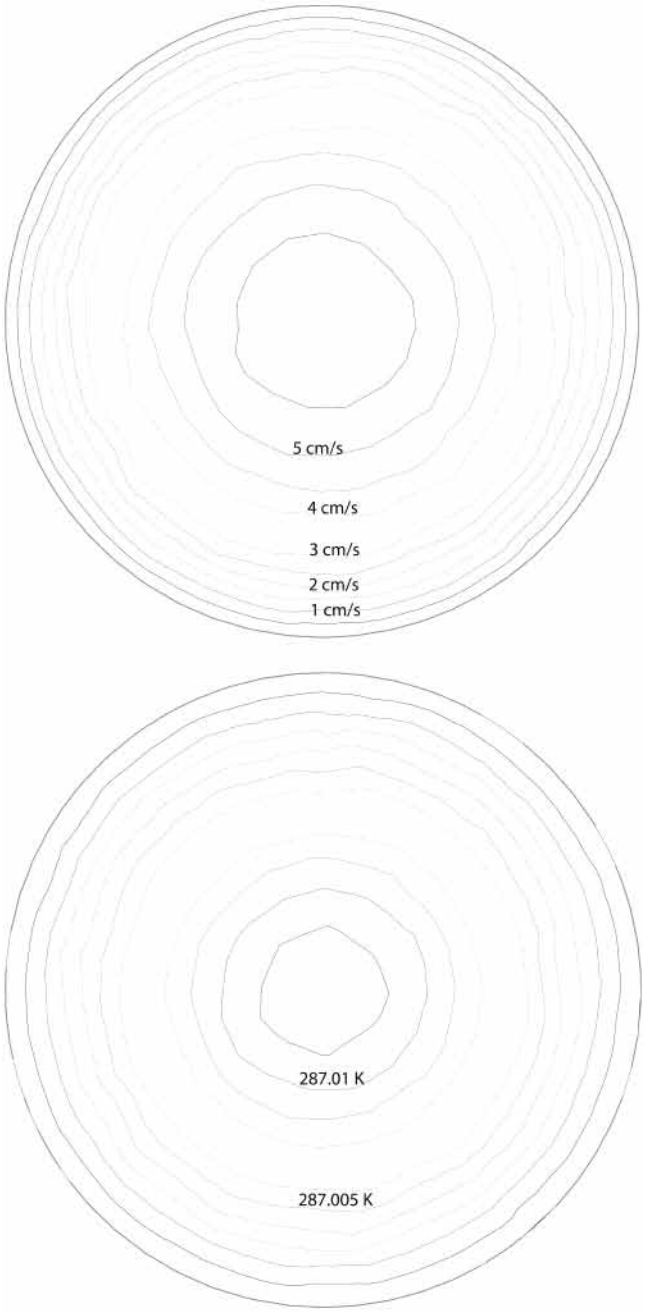

Figure A2. Results from computation fluid dynamics simulation of the flow reactor with the wall held at 287 K and the incoming gas at 295 K. Radial cross sections near the middle of the reactor are shown for (a) the axial flow velocity for 0.5 to 6 cm/s by 0.5 cm/s, and (b) temperature from 287.01 to 287 K with 0.001 K intervals.

Finally, we show that this effect plays no role in the present experiments. The aerosol particles are slightly cooled as they flow through the reaction region (see below). A cooling of ~0.04 K occurs in about 5 s and a further cooling of 0.01 K occurs in the last 5 s of transit through the reaction region. For the most dilute particles presented here, the composition changed from 15.4 to 15.0 wt % H_2SO_4 as the temperature was cooled from 287.05 to 287.0 K. This is a change in volume of ~2.7% and in radius of ~0.9% which is a change of 0.9 nm for $a =$ 100 nm. The net H_2O flux, averaged over 10 s, is then 3 $\times$

10^{14} molecule cm^{-2} s^{-1} and along with $n_T = 2 \times 10^{19}$ cm^{-3}, eq 12 gives an absorbent flux that is $\sim 10^{-5} \times n_s$, which is completely negligible.

Appendix C. Computational Fluid Dynamics of the Aerosol Flow Reactor. The flow in the reactor was numerically modeled using the Fluent fluid dynamics package.[50] The flow reactor was 120 cm long with a 5 cm inner diameter and the main gas inlet (a tube 10 cm long with a 0.4 cm i.d.) was aligned radially to the flow tube. There were approximately 5×10^5 volume elements. The calculation showed that the axial velocity V_z profile was that expected of laminar ($V_z(r) = 2V_{ave}(1 - (r/a)^2$ where V_{ave} is the average velocity and a is the reactor radius) to better than 8% over the entire length of the reaction region (the lower half of the flow reactor).

Calculations of the flow profile were also performed with the incoming gas at a temperature of 295 K interacting with the wall at a temperature of 287 K. A cross section of the flow reactor is shown in Figure A2 where the axial flow velocity (a) and temperature (b) are shown in contour plots for a slice of the flow reactor near the middle of the reaction region ($Z = 40$ cm). The temperature of the gas along the axis of the flow reactor was within 0.05 K of the wall by the time it reached the beginning of the reaction region (60 cm from the end) and was within 0.01 K of the wall by the time it was halfway through this region (Figure A2b).

This result has two important implications for the measurements where the flow reactor wall temperature was cooled: (1) the aerosol particles had attained a temperature very close to that of the wall, and (2) the assumption of laminar flow is valid. Because the gas (and thus the particles as they are $\sim 3 \times 10^{-8}$ in mass mixing ratio) attained the temperature of the wall to better than 0.01 K over most of the measurement region, the calculation of the surface area due to swelling (eq 11) gives the actual surface area of the particles to better than 1%. This uncertainty is negligible compared to the uncertainty (up to 10%) that was included in the data analysis due to the application of eq 11 and a relative temperature uncertainty of 0.2 K.

References and Notes

(1) Ball, S. M.; Hanson, D. R.; Eisele, F.; McMurry, P. M. *J. Geophys. Res.* **1999**, *104*, 23709.

(2) Hanson, D. R.; Eisele, F. *J. Geophys. Res. D* **2002**, *107*, 10.1029.

(3) Coffman, D. J.; Hegg, D. A. *J. Geophys. Res.* **1995**, *100*, 7147−7160. Korhonen, P.; Kulmala, M.; Laaksonen, A.; Viisanen, Y.; McGraw, R.; Seinfeld, J. H. *J. Geophys. Res.* **1999**, *104*, 26349−26353.

(4) Weber, R. J.; Marti, J.; McMurry, P. H.; Eisele, F. L.; Tanner, D. J.; Jefferson, A. *Chem. Eng. Commun.* **1996**, *157*, 53−64.

(5) Charlson, R. J.; Vanderpol, A. H.; Covert, D. S.; Waggoner, A. P.; Ahlquist, N. C. *Science* **1974**, *184*, 156.

(6) Finlayson-Pitts, B. J.; Pitts, J. N. *Atmospheric Chemistry*; John Wiley and Sons: New York, 1986; pp 790−799.

(7) Robbins, R. C.; Cadle, R. D. *J. Phys. Chem.* **1958**, *62*, 469.

(8) Huntzicker, J. J.; Cary, R. A.; Ling C.-S. *Environ. Sci. Technol.* **1980**, *14*, 819−824.

(9) McMurry, P. M.; Takano, H.; Anderson, G. R. *Environ. Sci. Technol.* **1983**, *17*, 347−352.

(10) Daumer, B.; Niessner, R.; Klockow, D. *J. Aerosol Sci.* **1992**, *23*, 315−325.

(11) Rubel, G. O.; Gentry, J. W. NH_3 + phosphoric acid particles. *J. Aerosol Sci.* **1984**, *15*, 661−671.

(12) Swartz, E.; Shi, Q.; Davidovits, P.; Jayne, J. T.; Worsnop, D. W.; Kolb, C. E. *J. Phys. Chem.* **1999**, *103*, 8824−8833.

(13) Klassen, J. K.; Nathanson, G. M. Personal communication, 2002.

(14) Lovejoy, E. R.; Hanson, D. R. *J. Phys. Chem.* **1994**, *99*, 2080.

(15) Mozurkewich, M.; Calvert, J. G. *J. Geophys. Res.* **1988**, *93*, 15889.

(16) Keyser, L. F. *J. Phys. Chem.* **1984**, *88*, 4750−4758, and references therein.

(17) Hanson, D. R.; Greenberg, J.; Henry, B. E.; Kosciuch, E. *Int. J. Mass Spectrom.*, in press.

(18) Lau, Y. K.; Ikuta, S.; Kebarle, P. *J. Am. Chem. Soc.* **1982**, *104*, 1462−1469.

(19) Viggiano, A. A.; Dale, F.; Paulson, J. F. *J. Chem. Phys.* **1988**, *101*, 2469−2477.

(20) Ellis, H. W.; McDaniel, E. W.; Albritton, D. L.; Viehland, L. A.; Lin, S. L.; Mason, E. A. *At. Data Nucl. Data Tables* **1978**, *22*, 179−217.

(21) Clegg, S. L.; Brimblecombe, P.; Wexler, A. S. *J. Phys. Chem. A* **1998**, *102* (2), 2137−2154, (http://www.uea.ac.uk/∼e770/aim. html).

(22) Fried, A.; Henry, B.; Calvert, J.; Mozurkewich, M. *J. Geophys. Res.* **1994**, *99*, 3517.

(23) Hanson, D. R.; Eisele, F. L.; Ball, S. M.; McMurry, P. M. *Aerosol Sci. Technol.* **2002**, *36*, 554.

(24) Gmitro, J. I.; Vermeulen, T. *AIChE.* **1964**, *10*, 7640.

(25) Fuchs, N. A.; Sutugin, A. G. H*ighly Dispersed Aerosols*; Ann Arbor Science: Ann Arbor, MI, 1970.

(26) Lovejoy, E. R.; Huey, L. G.; Hanson, D. R. *J. Geophys. Res.* **1995**, *100*, 18775.

(27) Brown, R. L. *J. Res. Natl. Bur. Stand. (U.S.)* **1978**, *83*, 1−8.

(28) Howard, C. J. *J. Phys. Chem.* **1979**, *83*, 3−9.

(29) (a) Worsnop, D. W., et al. *J. Phys. Chem.* **1989**, *93*, 1159. (b) Worsnop, D. W., et al. *J. Aerosol Sci.* **2001**, *32*, 877−891. (c) Gardner, J.; Watson, L.; Adewuyi, Y.; Davidovits, P.; Zahniser, M.; Worsnop, D.; Kolb, C. *J. Geophys. Res.* **1987**, *92*, 10887.

(30) Ponche, J. L.; George, C. H.; Mirabel, P. H. *J. Atmos. Chem.* **1993**, *16*, 1−22.

(31) Bongartz, A.; Schweighoefer, S.; Roose, C.; Schurath, U. *J. Atmos. Chem.* **1995**, *20*, 35.

(32) Van Doren, J. M.; Watson, L. R.; Davidovits, P.; Worsnop, D. R.; Zahniser, M. S.; Kolb, C. E. *J. Phys. Chem.* **1990**, *94*, 3265.

(33) Watson, L. R.; Van Doren, J. M.; Davidovits, P.; Worsnop, D. R.; Zahniser, M. S.; Kolb, C. E. *J. Geophys. Res.* **1990**, *95*, 5631.

(34) Van Doren, J. M.; Watson, L. R.; Davidovits, P.; Worsnop D. R.; Zahniser, M. S.; Kolb, C. E. *J. Phys. Chem.* **1991**, *95*, 1684.

(35) Robinson, G.; Worsnop, D. R.; Jayne, J. R.; Kolb, C. E.; Swartz, E.; Davidovits, P. *J. Geophys. Res.* **1998**, *103*, 25371.

(36) Hanson, D. R.; Lovejoy, E. R. *J. Phys. Chem.* **1996**, *100*, 6397.

(37) Rudolf, R.; Vrtala, A.; Kulmala, M.; Vesala, T.; Viisanen, Y.; Wagner, P. E. *J. Aerosol Sci.* **2001**, *32*, 913.

(38) Li, Y. Q.; Davidovits, P.; Shi, Q.; Jayne, J. R.; Kolb, C. E.; Worsnop, D. R. *J. Phys. Chem. A* **2001**, *105*, 10627.

(39) Wilson, M. A.; Pohorille, A. *J. Phys. Chem. B* **1997**, *101*, 3130.

(40) Taylor, R. S.; Ray, D.; Garret, B. C. *J. Phys. Chem. B* **1997**, *101*, 5473.

(41) Jayne, J. T.; Duan, S. X.; Davidovits, P.; Worsnop, D. R.; Zahniser, M. S.; Kolb, C. E. *J. Phys. Chem.* **1991**, *95*, 6329.

(42) Sugiyama, M.; Koda, S.; Morita, A. *Chem. Phys. Lett.* **2002**, *362*, 56−62. Morita, A.; Sugiyama, M.; Koda, S. *J. Phys. Chem.*, submitted.

(43) Shi, Q.; Davidovits, P.; Jayne, J. T.; Worsnop, D. W.; Kolb, C. E. *J. Phys. Chem.* **1999**, *103*, 8812−8823.

(44) Trautz, M.; Muller, W. *Ann. Physik* **1935**, *414*, 333. Wilke, C. R.; Lee, C. Y. *Ind. Eng. Chem.* **1955**, *47*, 1253.

(45) Andrew, S. P. S. *Chem. Eng. Sci.* **1955**, *4*, 269. Spiller, L. L. *Anal. Lett.* **1989**, *22*, 2561. Bongartz, A.; Schweighoefer, S.; Roose, C.; Schurath, U. *J. Atmos. Chem.* **1995**, *20*, 35.

(46) Jayne, J. T.; Worsnop, D. R.; Kolb, C. E.; Swartz, E.; Davidovits, P. *J. Phys. Chem.* **1996**, *100*, 8015.

(47) Perry, R. H.; Chilton, C. H. *Chemical Engineers Handbook*, 5th ed.; McGraw-Hill: New York, 1978.

(48) Covert, D.; Wiedensohler, A.; Russel, L. *Aerosol Sci. Technol.* **1997**, *27*, 206.

(49) Tang, I. N.; Munkelwitz, H. R. *J. Geophys. Res.* **1994**, *99*, 18801.

(50) *Fluent 5.5*; Fluent Inc.: Lebanon, NH, 2000.

(51) Schwartz, S. E. In *Chemistry of Multiphase Atmospheric Systems*; Jaeschke, W., Ed.; Springer-Verlag: New York, 1986.

(52) Mason, E. A.; Monchick, L. *J. Phys. Chem.* **1961**, *36*, 2746.